Identification and Validation of T-cell Receptors Targeting *RAS* Hotspot Mutations in Human Cancers for Use in Cell-based Immunotherapy

Noam Levin[1], Biman C. Paria[1], Nolan R. Vale[1], Rami Yossef[1], Frank J. Lowery[1], Maria R. Parkhurst[1], Zhiya Yu[1], Maria Florentin[1], Gal Cafri[1,2], Jared J. Gartner[1], Mackenzie L. Shindorf[1], Lien T. Ngo[1], Satyajit Ray[1], Sanghyun P. Kim[1], Amy R. Copeland[1], Paul F. Robbins[1], and Steven A. Rosenberg[1]

ABSTRACT

Purpose: Immunotherapies mediate the regression of human tumors through recognition of tumor antigens by immune cells that trigger an immune response. Mutations in the *RAS* oncogenes occur in about 30% of all patients with cancer. These mutations play an important role in both tumor establishment and survival and are commonly found in hotspots. Discovering T-cell receptors (TCR) that recognize shared mutated RAS antigens presented on MHC class I and class II molecules are thus promising reagents for "off-the-shelf" adoptive cell therapies (ACT) following insertion of the TCRs into lymphocytes.

Experimental Design: In this ongoing work, we screened for RAS antigen recognition in tumor-infiltrating lymphocytes (TIL) or by *in vitro* stimulation of peripheral blood lymphocytes (PBL). TCRs recognizing mutated RAS were identified from the reactive T cells. The TCRs were then reconstructed and virally transduced into PBLs and tested.

Results: Here, we detect and report multiple novel TCR sequences that recognize nonsynonymous mutant RAS hotspot mutations with high avidity and specificity and identify the specific class-I and -II MHC restriction elements involved in the recognition of mutant RAS.

Conclusions: The TCR library directed against RAS hotspot mutations described here recognize RAS mutations found in about 45% of the Caucasian population and about 60% of the Asian population and represent promising reagents for "off-the-shelf" ACTs.

Introduction

Most approaches to cancer immunotherapy, including adoptive cellular therapy (ACT), rely on T-cell target-specific recognition (1–3). Neoantigens, which are encoded by mutated genes that exist only in cancer cells, can be a good target for T cells (4–6). Administration of tumor-infiltrating lymphocytes (TIL) enriched with T cells, which recognize tumor-specific neoantigens, can mediate long-term objective responses in patients with various metastatic cancers, including complete remissions, which are dependent on specific T-cell receptor (TCR) recognition of the MHC–cancer antigen complex (6–17). Although the majority of cancer antigens are unique and specific only to the patients in which they are found (18), a relatively small group of mutations occurs at specific amino acid positions in genes that play a critical role in tumorigenesis, referred to as hotspot or driver mutations. Hotspot mutations in members of the *RAS* family represent proteins that are involved in the transduction of signals that are essential for tumor establishment and survival and therefore are likely to be clonally expressed in all tumor cells present in a patient with cancer (19, 20).

The incidence of *RAS* mutations varies with cancer histology; however, they are found in about 30% of all patients with cancer (20–23). Up to 94% of pancreatic cancers and up to 45% of colon cancers express a *RAS* mutation (19–21, 23–28). The human RAS super-family proteins (KRAS/NRAS/HRAS) have an identical amino acid sequence in positions 1 through 86 (20, 25), and more than 99% of all mutations in this gene family occur at positions 12, 13, or 61 (COSMIC database; ref. 29) within the domains responsible for GTP dephosphorylation into GDP, resulting in constitutive activation of the RAS protein (20–23, 25, 28, 30). Because these are gain-of-function mutations, one mutated allele expressed at normal level is sufficient to support cancer growth and establishment (22, 31, 32). Mutations in *RAS* predominantly occur in *KRAS* (85%), but also in *NRAS* or *HRAS* (11% and 4%, respectively). The most common mutations in KRAS are G12D (35%), G12V (24%), G13D (13%), G12C (12%), G12A (6%), G12S (5%), and G12R (3%; ref. 22). While a small molecule targeting the RAS^{G12C} mutation is currently being evaluated in patient clinical trials, there is no available treatment for other more common RAS hotspot mutations, such as G12D or G12V (33–35).

Previously, we have shown that ACT with TILs targeting a *KRAS* neoepitope, recognized in the context of the HLA-C*08:02 restriction element expressed by approximately 3% of the patient population, resulted in durable tumor regression in a patient with metastatic colon cancer, who is still alive and disease-free over 4 years later (17). In most patients bearing *RAS*-mutant tumors, screening of TILs has failed to result in the identification of mutant RAS–specific T cells, which is likely due to the low frequency of such T cells (18).

The administration of peripheral blood lymphocytes (PBL) virally transduced with genes encoding for TCRs or chimeric antigen

[1]Surgery Branch, National Cancer Institute, Bethesda, Maryland. [2]Sheba Medical Center, Ramat Gan, Israel.

Corresponding Author: Steven A. Rosenberg, Building 10, Room 3–3940, Bethesda, MD 20892-1201. Phone: 240-858-3080; E-mail: sar@nih.gov

Clin Cancer Res 2021;27:5084–95

doi: 10.1158/1078-0432.CCR-21-0849

Translational Relevance

Approximately 30% of all cancers comprising the most common malignancies possess a *RAS* hotspot mutation. In this article, we characterize a library of TCRs directed against mutant RAS epitopes that can potentially be used for the evaluation of TCR-based adoptive cell transfer therapies in the 45%–60% of patients where tumors bear *RAS* mutations.

receptors (CAR) can mediate regression of established cancers (36–40). Although specific TCRs recognizing RAS hotspot mutations could potentially be used in ACT as an "off-the-shelf" reagent in an allogeneic setting for patients whose tumors express the relevant hotspot mutation and appropriate MHC restriction element, there are few RAS hotspot mutation–reactive TCRs isolated from TILs reported in the literature (41, 42). The use of a patient's PBLs, which will be genetically engineered to express a specific anti-RAS TCR, has the potential advantage of generating highly enriched tumor-reactive cells in a less differentiated state than cells present in TILs. Here we describe the identification of multiple CD4 and CD8 T-cell reactivities targeting RAS hotspot antigens by TIL screening and *in vitro* stimulation (IVS) of PBLs from patients with cancer harboring a *RAS* mutation in their tumor. We report the TCR sequences and cognate MHC restrictions of a validated TCR library targeting products of *RAS* mutations with little to no reactivity against wild-type (WT) RAS. This library has the potential to treat about 45% of the Caucasian population and about 60% of the Asian population in the United States bearing *RAS*-mutant cancers.

Materials and Methods

Cell media and reagents

The following media and buffers were used: RPMI1640, DMEM, AIM-V, PBS, and Opti-MEM. The following media supplementary materials were used: penicillin and streptomycin (Pen/Strep), L-glutamine, HEPES buffer saline, gentamicin, MEM nonessential amino acid, and 2-mercaptoethanol (all purchased from Gibco, Thermo Fisher Scientific), ethylenediaminetetraacetic acid (EDTA; Corning), human AB serum (Valley Biomedical, Inc), FBS (Sigma-Aldrich), recombinant IL2 (Prometheus), recombinant IL4 (PeproTech), and recombinant GM-CSF (Leukine).

RPMI complete media was comprised of RPMI1640 supplemented with 5% human AB serum, 100 U/mL penicillin, 100 μg/mL streptomycin, 2 mmol/L L-glutamine, 25 mmol/L HEPES, and 10 μg/mL gentamicin.

Dendritic cell (DC) media was comprised of RPMI complete media supplemented with 800 IU/mL GM-CSF and 200 U/mL IL4.

Tissue culture media was comprised of RPMI1640 supplemented with 10% FBS, nonessential amino acid, 1 mmol/L sodium pyruvate, 100 U/mL penicillin, 100 μg/mL streptomycin, 2 mmol/L L-glutamine, 10 μg/mL gentamicin, and 55 μmol/L 2-mercaptoethanol.

Cell line media was comprised of DMEM containing 10% FBS, 100 U/mL penicillin, 100 μg/mL streptomycin, 12.5 mmol/L HEPES, 110 mg/mL sodium pyruvate, and 2 mmol/L L-glutamine.

T-cell media was comprised of a 1:1 mix of RPMI1640 and AIM-V supplemented with 5% human AB serum, 2 mmol/L L-glutamine, 100 U/mL penicillin, 100 μg/mL streptomycin, 12.5 mmol/L HEPES, 10 μg/mL gentamicin, and 5% human serum. Unless otherwise noted, TILs were grown in T-cell media supplemented with 3,000 IU/mL IL2 and PBLs were grown in T-cell media supplemented with 300 IU/mL IL2.

FACS buffer was comprised of sterile PBS, 1% FBS, and 2 mmol/L EDTA.

Freezing media was comprised of 90% FBS and 10% DMSO.

All media were 0.22 μm filtered.

Antibodies, flow cytometry, and cell sorting

The antimouse TCRβ (mTCR)- PerCp-Cy5.5, CD8a-eFluor 450, were purchased from eBioscience. CD3-APC-Cy7, CD4- PE/FITC/APC, 41BB- APC/PE, CD8- PE-Cy7/FITC, OX40- FITC/PE-Cy7, CD62L-PE, and CD45RO-APC/BV421 were purchased from BD Biosciences. CD3-Alexa Fluor 700, CD62L-PE-Cy7, and the live/dead stains- DAPI/PI were purchased from BioLegend.

For FACS sample preparation, cells were harvested and washed with FACS buffer. Cells were resuspended in FACS buffer at a concentration of 1–50 $\times$ 10^6 cells/mL and extracellular fluorescence-conjugated primary antibodies were added and mixed in. After a 20- to 60-minute incubation at 4°C, which was also protected from light exposure, the samples' cells were washed and resuspended with FACS buffer.

The flow cytometry assays were performed on FACSCanto I/II (BD Biosciences) and the acquired data were analyzed with FlowJo software (TreeStar). Cells were sorted to: Live/$CD3^+$, separated for $CD4^+$ or $CD8^+$, $T_{EMRA}/T_{EM}/T_{CM}$ based on sorting out $CD62L^+/CD45RO^-$ (naïve T cells). Cocultures were sorted for enrichment or into single reactive cells based on $41BB^+/OX40^+$ (both double- and single-positive cells), Live/$CD3^+$, separated for $CD4^+$ or $CD8^+$ by SH800S/MA900 instrument (Sony Biotechnology) or by FACSAria II (BD Biosciences).

Construction of genes, peptides, and *in vitro* transcription

The amino acid sequences from peptides used are shown in Supplementary Fig. S1. Minimal epitope (ME) sequence predictions were generated for RAS-mutated sequences (NetMHC/4.0) and ME (9–12 amino acids short peptides) predicted to attach to common MHC-I or to multiple MHCs. Peptides with predicted binding affinity percentage ranks of less than 0.5 are generally denoted as strong binders while peptides with ranks of between 0.5 and 2 are denoted as weak binders. Long peptides (LP) were 24–25-mer, designed with the mutated amino acid in the middle, and 12 normal amino acids upstream and downstream. LPs were ordered for RAS hotspot mutations found in more than 0.5% of patients with RAS-mutated cancer (G12D, G12V, G12C, G12A, G12S, G13D, G13R, G13V, Q61R, Q61L, Q61K, and Q61H) and the equivalent WT (G12, G13, Q61). All peptides were ordered from GenScript or JPT and were HPLC purified (>90%). For tandem minigenes (TMG) construction, each *RAS* hotspot mutation and the equivalent WT minigene encoding the same LP sequences were composed sequentially into one gene (Supplementary Fig. S1) and cloned into the pcRNA2SL-GFP plasmid. Full-length (FL) *RAS* genes encoding to the mutated or wild type *KRAS* were synthesized and cloned into pcRNA2SL-GFP using *Eco*RI and *Bam*HI. Gene synthesis and cloning was done by GenScript. For mRNA *in vitro* transcription (IVT), we used mMessage mMachine T7 Ultra kit (Thermo Fisher Scientific) and all procedures were followed as per the manufacturer's instructions. Briefly, the pcRNA2SL constructed plasmids were linearized with *Not*-I restricted enzyme, followed by ethanol precipitation. Next, we used 1 μg of linearized DNA to generate IVT mRNA. The mRNA was ethanol precipitated and resuspended at 1 μg/μL.

Generation of TILs

TILs were generated as described elsewhere (18, 43). For details, see Supplementary Materials and Methods.

Generation of antigen-presenting cells

Immature DCs were generated in the laboratory using a standard protocol of adherence method. Apheresis samples were thawed, washed, set to 5–10 $\times$ 10^6 cells/mL with AIM-V media (Life Technologies), and 1.75–2 $\times$ 10^8 viable cells were incubated in T175 flasks (Corning Inc.) at 37°C. After 2 hours, the flasks were washed two to three times vigorously with sterile PBS to collect nonadherent cells for T-cell sorting. For the adherent cells, 30 mL DC media were added, and cells were incubated at 37°C, 5% CO_2. On day 4 or 5, cells were harvested and used or frozen for further use. DCs were seeded into low-attachment 96-, 12-, or 6-well plates for peptide loading with 0.1–10 μg/μL peptide for 2 to 12 hours at 37°C, 5% CO_2. Alternatively, mRNA transfection with TMG or FL was done with mMessengerMAX reagent (Life Technologies) according to the manufacturer's instructions, and cells were incubated for 8 to 20 hours at 37°C, 5% CO_2. Before the coculture experiment (for analysis/sorting/IVS), DCs were harvested by washing twice with 0.9 mmol/L EDTA in PBS. DCs were resuspended in T-cell media at a concentration of 2.5 $\times$ 10^5–1 $\times$ 10^6 cells/mL.

Memory T-cell preparation

Nonadherent cells [from the antigen-presenting cells (APC) protocol] were spun down, resuspended in T-cell medium, and rested overnight at 37°C, 5% CO_2. Cells were prepared and sorted (as described above) for T memory ($T_{EMRA}/T_{EM}/T_{CM}$) cells. Sorted CD4 or CD8 T memory cells were collected, counted, and washed. T cells were resuspended in T-cell medium containing 60 ng/mL IL21 at a concentration of 2 $\times$ 10^6 cells/mL.

IVS to memory T cells

This method is published in detail elsewhere (41). For details, see Supplementary Materials and Methods.

Coculture screening assays: IFNγ ELISpot, ELISA, and flow cytometry for OX40 and 41BB activation markers' staining

DCs or cell-line cells were used as target cells, with 3 $\times$ 10^4–1 $\times$$10^5$ cells/well in 96-well plates. Effector T cells (2 $\times$ 10^4–5 $\times$ 10^4 cells/well) were used in 96-well plates. All cocultures were performed in T-cell media in the absence of exogenously added cytokines. Phorbol 12-myristate 13-acetate: ionomycin mixture (eBioscience) or CD28/CD3 Dynabeads (Thermo Fisher Scientific) were used as a positive control. In HLA-blocking assays, target cells were incubated with 20–50 μg/mL blocking antibodies for 2 hours at 37°C, 5% CO_2, and then effector cells were added and incubated for 12 to 18 hours. IFNγ ELISpot assays were performed in MultiScreen-IP filter plates (EMD Millipore). Each plate was pretreated with 50 μL 70% ethanol/well for less than 2 minutes, washed three times with PBS and then coated with 10 μg/mL of an IFNγ capture antibody (60 μL/well, clone: 1-D1K, Mabtech, diluted in PBS) overnight at 4°C. At the day of coculture, each plate was washed three times with PBS and blocked with complete media without IL2 for 2 hours at room temperature. After overnight coculture (18–24 hours), the cells were harvested and transferred into a round-bottom 96-well plate for flow cytometry staining and analysis. Each ELISpot plate was washed five times with PBS containing 0.05% Tween 20 (MP Biomedicals) and then incubated for 2 hours with 1 μg/mL, 0.22 μmol/L-filtrated antihuman-IFNγ detection antibody (clone: 7-B6–1, Mabtech, 100 μL/well, diluted in PBS + 0.5% FBS). Next, each plate was washed five times with PBS containing 0.05% Tween 20 and incubated for 1 hour with streptavidin-ALP (Mabtech, 100 μL/well, 1:3,000 diluted with PBS + 0.5% FBS), followed by three washes with PBS and development with 0.45-μm–filtered 5-bromo-4-chloro-3-indolyl phosphate (BCIP)–nitroblue tetrazolium (NBT) substrate solution (KPL, 100 μL/well) for 5 to 15 minutes. The reaction was stopped by rinsing thoroughly with cold tap water. After the plates dried completely, each ELISpot plate was scanned and counted using an ImmunoSpot plate reader and associated software (Cellular Technologies Limited). The harvested cells from the coculture ELISpot wells prior to IFNγ spot development were spun down and the media discarded. Cells were resuspended in the remaining liquid and stained for flow cytometry and surface expression of 41BB and OX40 in Live/$CD3^+$, $CD4^+$ or $CD8^+$, and $mTCR^+$ (when iTCR was tested in the experiment) was assessed using BD FACSCantoI or BD FACSCantoII (BD Biosciences). All flow cytometry data were analyzed using FlowJo software (TreeStar Inc). Cell media were analyzed to IFNγ by human IFNγ Duoset ELISA (R&D Biosystems) and completed as the protocol instructed.

Reactivity was defined by a higher percentage of cells either: expressing 41BB and/or OX40 or demonstrating an increased number of spots in the IFNγ ELISpot when the RAS mutated antigen was tested in comparison to the WT and DMSO. Reactivity could be in the gene (FL/TMG), the LP levels, or in both.

Single-cell sorting and single-cell RT-PCR

T cells were sorted to single-cell cultures by identifying their reactivity as reflected by the expression of 41BB/OX40 above the background to target cells (single- or double-positive) as described previously (44, 45). Cells were sorted into a 96-well plate containing RT-PCR buffer (CellsDirect One-Step qRT-PCR kit, Thermo Fisher Scientific), with each well containing one primer to the Cα and Cβ regions (1.2 μmol/L for these gene-specific RT primers) and multiple Vα and Vβ primers (0.6 μmol/L) in 10 μL volume. Cycling conditions were: 50°C for 15 minutes, 95°C for 2 minutes, and 18 cycles of 95°C for 15 seconds, 55°C for 30 seconds, and 72°C for 1 minute. The second PCR was performed separately for TCRα and TCRβ chains. Platinum II Hot-Start PCR master mix (2X) was used for both PCRs for a total of 25 μL volume that included 2.5 μL of the RT-PCR mix with several nested primers (0.6 μmol/L each) for either TCRα or TCRβ targeting the extended CDR3 regions of both chains. The PCR programs were: 95°C for 7 minutes, 5 cycles of 95°C for 15 seconds, 65°C for 15 seconds, and 72°C for 30 seconds, followed by 5 cycles of 95°C for 15 seconds, 60°C for 15 seconds, and 72°C for 30 seconds. This was followed by 40 cycles of 95°C for 15 seconds, 65°C for 15 seconds, and 72°C for 30 seconds; then incubation at 72°C for 7 minutes; and finally incubation at 4°C. The PCR products were purified and sequenced by Sanger methods within internally nested Cα and Cβ region primers (Beckmann Coulter).

TCR reconstruction and subcloning into a retroviral vector

The Sanger sequencing method produced sequencing data that contained the 3′ end of the variable region and the full CDR3 region of matching TCRα and TCRβ genes. The data were analyzed using IMGT/V-Quest tool (http://www.imgt.org/IMGT_vquest/vquest). The pairing methods used herein are described elsewhere (16, 46, 47) and are further explained at Supplementary Materials and Methods. The full iTCR construct was cloned into a pMSGV1 retroviral vector.

T-cell transduction

T-cell stimulation was done by thawing autologous or healthy donor apheresis nonadherent cells (from the APC protocol), resuspended in

T-cell medium and rested overnight at 37°C, 5% CO_2. Cells were harvested and stimulated by concentrating 3.75×10^6 cells/mL in T-cell media containing 50 ng/mL soluble OKT3 (Miltenyi Biotec) and 300 IU/mL IL2 (Chiron), and every 2 mL (7.5×10^6 cells) were seeded in a single well of a 24-well plate for 2 days. Retroviral supernatants were generated (44) by seeding 2 mL of 6×10^5 cells/mL (cell line medium) HEK-293GP packaging cell line in 6-well poly-D-lysine–coated plates. After 24 hours, the media were changed to 2 mL cell line media without antibiotic. HEK293 GPs were cotransfected with 2 μg/well pMSGV-1 cloned plasmid and 1.4 μg/well envelope-encoding plasmid RD114 using Lipofectamine 2000 (Life Technologies). Retroviral supernatants were collected 48 hours later and then centrifuged onto Retronectin-coated (20 μg/mL; Takara) nontissue culture-treated 6-well plates at 2000 G for 2 hours at 32°C. Stimulated T cells were then washed, concentrated (2×10^6 per well at 0.5×10^6 cells/mL in IL2 containing T-cell media), and spun onto the retrovirus plates for 10 minutes at 1,500 rpm with the acceleration and brake set at 1. After 12 to 48 hours of incubation at 37°C, 5% CO_2, the cells were removed from the plates and further cultured in rIL2 containing T-cell media. GFP and mock transduction controls were included in transduction experiments. The TCR transduction efficacy was confirmed by using mouse TCRβ antibody 8 to 16 days after day of stimulation. The transduced TCR was tested in reactivity and avidity experiments.

TCR survey and deep sequencing

TCR-Vβ deep sequencing was performed by immunoSEQ (Adaptive Biotechnologies) on genomic DNA isolated from peripheral blood T cells and frozen tumor tissues. T-cell numbers in sequenced samples ranged from approximately 2×10^4 to 1×10^6 cells. TCRβ chain clonality and productivity were analyzed using immunoSEQ Analyzer 3.0 (Adaptive Biotechnologies). Only productive TCR rearrangements were used in the calculations of TCR frequencies.

Patient-derived xenografts

Fresh tumor tissues from patients were mechanically separated into fragments of 2 mm in dimension. One fragment was then implanted subcutaneously at the flank of an NOD/SCID gamma (NSG) mouse using a 20-gauge needle. Tumor growth was monitored weekly. Patient-derived xenografts (PDX) were harvested when their sizes were greater than 1 cm in dimension.

Tumor cell line derived from PDXs

Freshly harvested PDXs were cut into small fragments and placed in GentleMACS c-tubes containing 20 mL of tissue culture media. The tumor cells were then mechanically dissociated by GentleMACS dissociator (Miltenyi Biotec) using the "mouse implanted tumor 1.01" program. The resulting cell suspension was run through a 100-μm cell strainer and washed once with culture media before being placed in tissue culture flasks. Media were refreshed every 3 to 7 days and cells were split when confluence reached 70%. The PDX-derived tumor cell lines were characterized in more detail in the Supplementary Materials and Methods.

Coculture of PDX-derived tumor cells with neoantigen-specific TCR-transduced T cells

One day prior to coculture, tumor cells were placed into a 96-well plate in concentration of 1×10^5 cells in 200 μL of culture media per well. On the day of assay, 100 μL of fresh culture media with or without peptides was added. T cells (1×10^5 cells in 100 μL of culture media) were added to the tumor cells. The coculture was incubated at 37°C, 5% CO_2 for 16 hours. Supernatants from the coculture wells were collected from IFNγ ELISA and nonadherent cells were harvested for surface 41BB and OX40 marker detection by FACS.

Results

We prospectively tested TILs from 20 patients with gastrointestinal cancer enrolled in clinical trials at the NCI Surgery Branch over the last 2 years whose tumors expressed *RAS* mutations. The general scheme for identifying and validating TCRs targeting RAS hotspot mutations is shown in **Fig. 1**. Briefly, to identify T-cell reactivity against RAS hotspot mutations, patient TILs were cocultured with APCs either transfected with IVT RNAs or pulsed with 24- or 25-mer LPs flanked on either side of the hotspot mutation with 11 or 12 residues from the normal RAS protein sequence (Supplementary Fig. S1A). The IVT RNAs encoded either the FL mutant, the FL WT *KRAS* gene, TMG encoding 12 of the RAS hotspot mutations or corresponding WT residues (Supplementary Fig. S1A and S1B). Generally, LPs were more efficient at detecting CD4 reactivities and transfected IVT RNA was more efficient for the detection of reactive CD8 T cells (18). To test CD8 T-cell reactivity, we also used a library of predicted ME peptides from the RAS mutations for common MHC-I using the prediction algorithm NetMHC 4.0 (DTU Bioinformatics; Supplementary Fig. S1C). As positive controls, we took advantage of an HLA-A*11*01–restricted mouse TCR recognizing RAS^{G12D} and the human HLA-A*11:01–restricted TCR recognizing RAS^{G12V} that our group previously reported (refs. 41, 48; Supplementary Fig. S2.). Reactivity was tested by IFNγ secretion and by 41BB and OX40 coreceptors upregulation. Although, we always tested and gated for both 41BB and OX40 upregulation, as expected, 41BB upregulation usually detects CD8 reactivity and OX40 upregulation usually detects CD8 reactivity.

Identification of anti-RAS T-cell reactivity from TIL

As an example of this approach, 24 tumor fragments dissected from a metastatic colon cancer deposit from patient 4391 that expressed the $KRAS^{G12V}$ mutation were initially cultured in the presence of IL2 as described previously (49). Lymphocytes generated from these fragments were subsequently cocultured with autologous DCs loaded with RAS peptides/IVT RNA (**Fig. 2**). One TIL fragment (F1) demonstrated reactivity against RAS^{G12V} based on the upregulation of 4–1BB and OX40 (**Fig. 2A** and **B**) and by ELISpot measuring IFNγ secretion levels (**Fig. 2C**).

A prediction algorithm (NetMHCpan4.0) was then used to identify candidate MEs from RAS^{G12V} potentially able to bind to the HLA class I restriction elements (RE) present in patient 4391 (**Fig. 2D**). In addition to the VVGAVGVGK and VVVGAVGVGK peptides, previously shown to be recognized in the context of HLA-A*11:01 (48), the AVGVGKSAL peptide (ME8) was predicted to be a weak binder to C*01:02 and the peptide GAVGVGKSA was predicted to bind weakly to HLA-B*55:01 (**Fig. 2E**). When F1 was tested against DCs loaded with RAS^{G12V} MEs (listed in Supplementary Fig. S3A), reactivity was found against ME8 (**Fig. 2F**; Supplementary Fig. S3B). Reactivity was also detected against the RAS^{G12V} LP but not the RAS^{WT} LP (**Fig. 2F**). To identify the RE responsible for presentation of the RAS ME8 peptide, F1 TILs were cocultured with peptide-pulsed COS7 cells that had been transfected individually with plasmids to encoding the patient's HLA class I alleles. The results demonstrated that COS7 cells expressing HLA-C*01:02 but not any of the additional HLA REs expressed by patient 4391 were recognized by TIL F1 T cells that had been pulsed with the ME8 peptide or the RAS^{G12V} LP (**Fig. 2G**). To evaluate the avidity of the recognition, TIL F1 was cocultured with

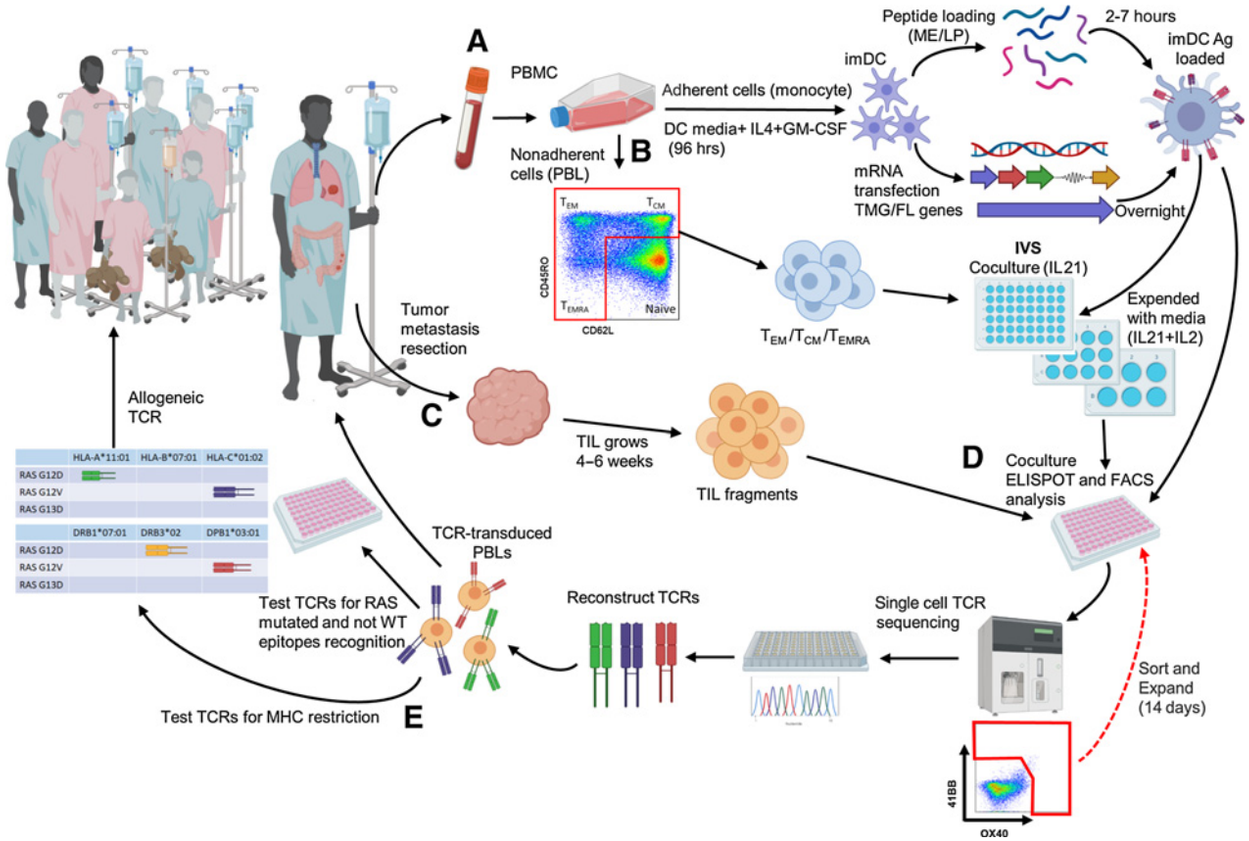

Figure 1.
Identification and validation of RAS hotspot mutation–reactive T cells from cancer patients with *RAS* mutations. **A,** Patient apheresis is collected. The blood is separated into adherent cells that are used to generate immature DCs (imDC). The imDCs are loaded with short predicted ME or with LP or are transfected with mRNA of the FL gene of the specific *RAS* mutation or with TMG containing all the common (more than 0.5%) RAS mutations. These Ag-loaded DCs are used for activating and testing T cells in all stages. **B,** Nonadherent cells (PBLs) are sorted into CD4 or CD8 T (CD3), central/effector memory (T_{CM}/T_{EM}), or effector (T_{EMRA}) cells (excluding naïve T cells) by using CD45RO and CD62L. This subset is used for IVS with RAS Ag-loaded DCs by coculture for 3 days with IL21 and then expanded with media containing IL21+IL2 every 2 days. Cells are restimulated and sorted for high expression of 41BB/OX40 and rapidly expanded (REP) for another 14 days. **C,** Tumor metastases are resected and cut into 24 fragments. TILs collected from each fragment are expanded in media containing IL2 until there are enough cells for testing (usually about 4–6 weeks). **D,** T cells are tested for reactivity to RAS mutations by IFNγ ELISpot, and 41BB/OX40 flow cytometry assays. The positive cultures are sorted to enrich the RAS reactive cells and then single cells are sequenced. The TCRs are reconstructed (iTCR) using mouse constant TCR elements to enhance the iTCR α/β pairing. The iTCR are transduced into autologous/healthy donor PBLs and tested for specific RAS-mutated and WT reactivity. Specific RAS-mutated TCRs with good avidity could then be used to treat the patient (as neoantigen treatment). **E,** After identifying the MHC restriction, the TCR could potentially be used to treat other patients having the same RAS mutation and MHC. All TCRs are saved in a library as prepared GMP vectors.

autologous DCs loaded with different peptide concentrations. Recognition of the ME8 peptide by TIL F1 was seen in concentrations as low as 10 ng/mL based on IFNγ ELISpot (Supplementary Fig. S3C). To identify TCR(s) reactive with the RAS^{G12V} C*01:02 epitope, F1 T cells that had been stimulated with DC transfected with the mutated TMG, were sorted for single-cell sequencing which revealed one functional TCR. The TRA and TRB chain sequences (TCR data in Supplementary Table S6) were cloned into the MSGV1 retroviral vector, which was then used to generate transient retroviral supernatants, which were used to virally transduce into healthy donor PBLs. The resulting bulk population was then evaluated for its ability to recognize DCs pulsed with the ME8 and corresponding WT peptides. On the basis of IFNγ ELISpot, the TCR recognized the mutated ME-loaded cells at concentrations as low as 10 ng/mL, similar to the minimum concentration recognized by TIL F1 T cells (**Fig. 2H**). Although the transduced cells were not separated into CD4 and CD8, the reactivity appeared to be at least partially CD8 coreceptor dependent as shown by FACS analysis of the gated populations (Supplementary Fig. S3D and S3E). Although the TCR was isolated from TILs, there was a potential risk that the TCRs recognizing the synthetic peptides/TMG would not recognize the tumor or would cross-react to an unknown antigen expressed in normal tissues. In an attempt to address this potential issue, 4391-TCR–transduced cells were tested for recognition against multiple tumor cell (TC) lines that either did or did not express HLA*C01:02 or RAS^{G12V}. TCR-transduced cells only recognized xenograft cell lines from patients 4391 and 4385, both of which expressed HLA-C*01:02 and RAS^{G12V}, but not six additional cell lines that lacked expression of either RAS^{G12V} or HLA-C*01:02. Pulsing the 4391 and 4385 TC lines with the ME8 peptide further enhanced recognition of the lines by 4391-TCR–transduced T cells, and in addition led to recognition of 4327, a colorectal TC line that expressed HLA-C*01:02 but not the RAS^{G12V} mutation (**Fig. 2I**; Supplementary Fig. S3F and S3G).

Similar analyses were carried out in other patients with tumors bearing *RAS* mutations. Screening of TIL fragment cultures from

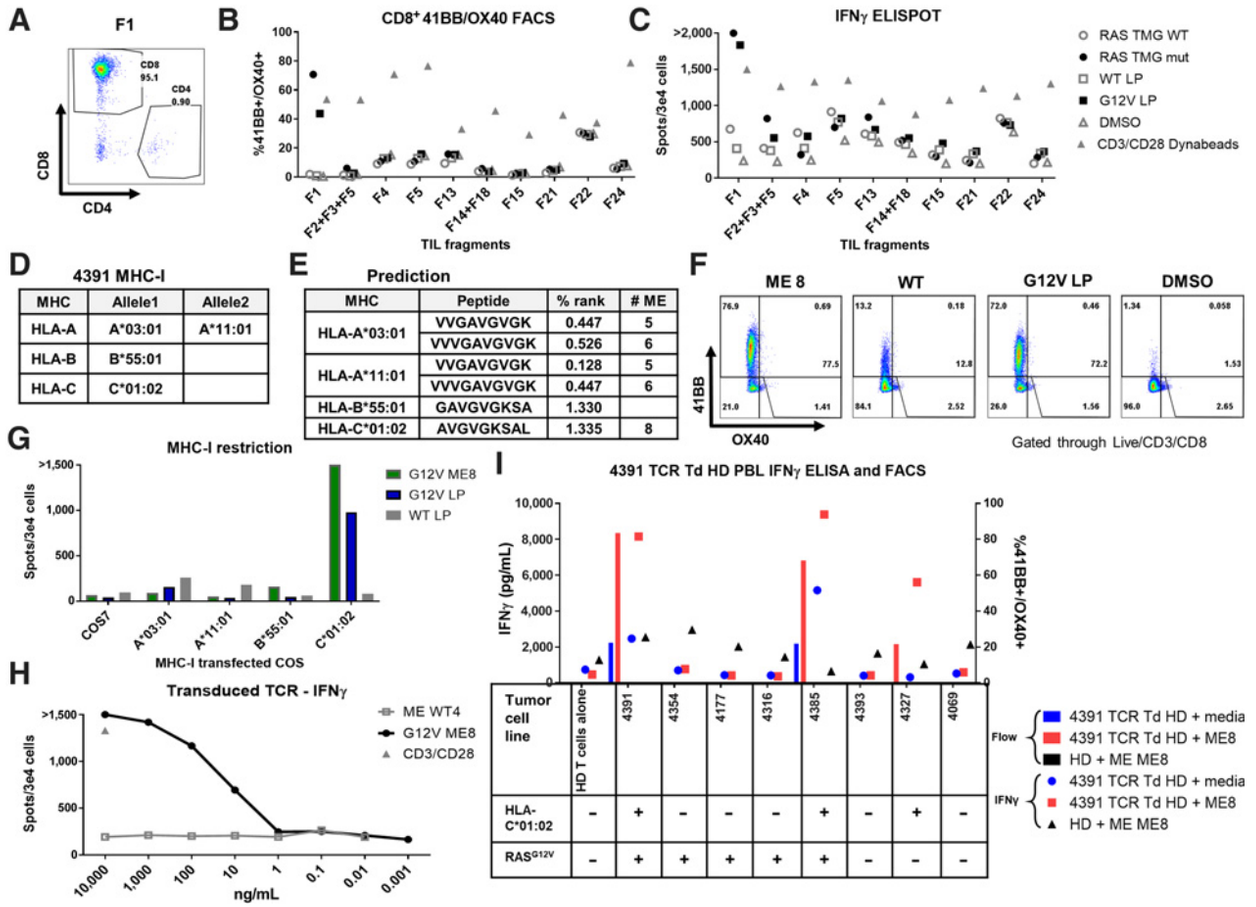

Figure 2.

TCR-recognized RAS^{G12V} hotspot mutation discovered by TIL screening. TIL fragments were screened for reactivity against autologous DCs transfected with *RAS* TMG (WT/Mutated) or loaded with 24-mer long peptide (RAS^{G12V}/RAS^{WT}). Coculture with DCs loaded with DMSO was used as a negative control. Anti-CD28/CD3 beads were used as a positive control. **A,** Most fragments, after gating on the live/CD3$^+$ cells and including fragment 1 (F1), primarily contained CD8$^+$ cells. Fragment reactivity tested in flow cytometry assays measured upregulation of 41BB$^+$ and OX40$^+$ (**B**) or by IFN-γ ELISpot (**C**). **D,** Table containing the patient 4391 MHC-I restriction elements. **E,** Table with the best-predicted RAS^{G12V} minimal epitopes (low % rank) to bind to the patient MHCs by the NetMHC 4.0. **F,** To determine which ME is recognized by TIL F1, cells were cocultured with autologous DC preloaded with RAS^{G12V} ME8, with LP (RAS^{G12V}/RAS^{WT}), or with DMSO at an equivalent concentration. Reactivity was determined by upregulation of 41BB and OX40 surface markers in live/CD3$^+$/CD8$^+$ by flow cytometry. **G,** For testing the MHC-I restriction element, TIL F1 were cocultured with COS7 cells pretransfected with patient's class I HLA DNA plasmids and loaded with LP (RAS^{G12V}/RAS^{WT}) or ME8. Reactivity was determined by IFNγ ELISpot. One TCR was identified from patient 4391 TIL fragment F1 after single-cell sequencing. This TCR was virally transduced to healthy donor (HD) PBLs. **H,** The TCR avidity was tested in the transduced cells by coculture with DCs loaded with different concentrations of RAS^{G12V}/RAS^{WT} 9-mer ME8 or the equivalent WT sequence WT4. The cells were tested via IFNγ ELISpot, with anti-CD28/CD3 beads used as a positive control. **I,** The TCR specificity and tumor recognition tested by coculturing the TCR-transduced HD cells with different TC lines with or without (±) RAS^{G12V} and HLA-C*01:02. TC lines were loaded with RAS^{G12V} ME8, or not peptide-loaded (media). Unloaded TC lines expressed their native peptidomes (including RAS^{G12V}). The reactivity was tested by IFNγ ELISA and by flow cytometry assay for 41BB/OX40 surface marker upregulation in live/CD3$^+$/mTCR$^+$/CD8$^+$ cells. Untransduced HD loaded with ME8 was used as a negative control.

patient 4385 TIL demonstrated that Fragment 11 also recognized RAS^{G12V} in the context of HLA-C*01:02 (Supplementary Fig. S4A–S4I). The single dominant TCR identified from the reactive fragment was then cloned into the MSGV1 recombinant retroviral construct, and transient retroviral supernatants used to transduce healthy donor PBLs. The results of a peptide titration assay demonstrated that the TCRs from patient 4385 possessed a similar avidity as the TCRs isolated from 4391 (Supplementary Fig. S4E–S4M). In addition, patient 4373 TIL Fragment 8 recognized the RAS^{G12D} (Supplementary Fig. S5A), and PBLs transduced with TCR-2 isolated as described above were reactive to RAS^{G12D} in the context of HLA-A*11:01 (Supplementary Fig. S5B). Peptide titration assays indicated that TCR recognized the RAS^{G12D} 10-mer VVVGADGVGK at a minimal concentration of 1 ng/mL, but recognized the 9-mer VVGADGVGK at approximately 1,000 fold higher concentration (Supplementary Fig. S5C and S5D). Finally, CD4 reactivity against RAS^{G13D} was detected in patient 4400 TIL fragments (Supplementary Fig. S6A–S6C). From six isolated TCRs, two specifically recognized RAS^{G13D} (Supplementary Fig. S6D–S6F) in the context of HLA-DQA1*05:01/HLA-DQB1*03:01 (Supplementary Fig. S7A and S7B) at a minimum concentration of 1 ng/mL (Supplementary Fig. S7C–S7F). Overall screening of TIL fragments from 20 patients with tumors bearing *RAS* mutations for anti-RAS reactivity demonstrated reactivity in 25% (5/20) of the screened patients and in 2.2% (8/370) of total fragments screened (Supplementary Table S1).

Identification of anti-RAS T-cell receptors from PBLs

Recently, we demonstrated that reactivities that were not readily detected by screening TIL could be detected by stimulating patient's PBL using DCs presenting the mutated antigens (41, 50, 51). This IVS was required due to the low frequency of neoantigen-specific T cells in the blood. On the basis of studies of the sequence of the V-β chain of human TCR, these reactive T cells can be as rare as 0.001% in PBLs and can be below the threshold of detection of our reactivity test (51). We used this method to search for additional RAS-specific TCRs directed against nonsynonymous *RAS* mutations from patients' PBL. Initial screening of TIL fragments from colorectal cancer patient 4360 whose tumor bore a RAS^{G12V} failed to demonstrate reactivity against the mutated RAS long peptide or minigene antigen (Supplementary Fig. S9). PBL [(nonadherent peripheral blood mononuclear cells (PBMC)] collected by apheresis were subject to IVS by a method (**Fig. 1B**) involving electronic sorting of the T_{CM}, T_{EM}, and T_{EMRA} populations of the patient's bulk PBL (41). Sorted T cells were cocultured with autologous DC loaded with RAS antigens for 14 days and screened for reactivity by flow cytometry following antigen stimulation (**Fig. 3A**). T cells upregulating 41BB and OX40 costimulatory molecules following RAS^{G12V} LP IVS that had been sorted and subjected to a rapid expansion protocol (REP) and were then tested for reactivity. CD4 reactivity against the mutated LP and lesser reactivity against the WT peptide were seen (**Fig. 3B** and **C**). Following IVS with the RAS^{G12V} LP recognized DCs loaded with the mutant RAS^{G12V} LP down to a concentration of 100 pg/mL. Although the RAS^{WT} LP was recognized at a minimal concentration of 10 ng/mL, reactivity against RAS^{G12V} LP was higher in all concentrations except 10 μg/mL, indicating specificity for the mutant neoepitope (**Fig. 3D** and **E**).

To identify the MHC-II restriction elements recognized by the reactive cells, the cells following LP IVS were cocultured with COS7 cell

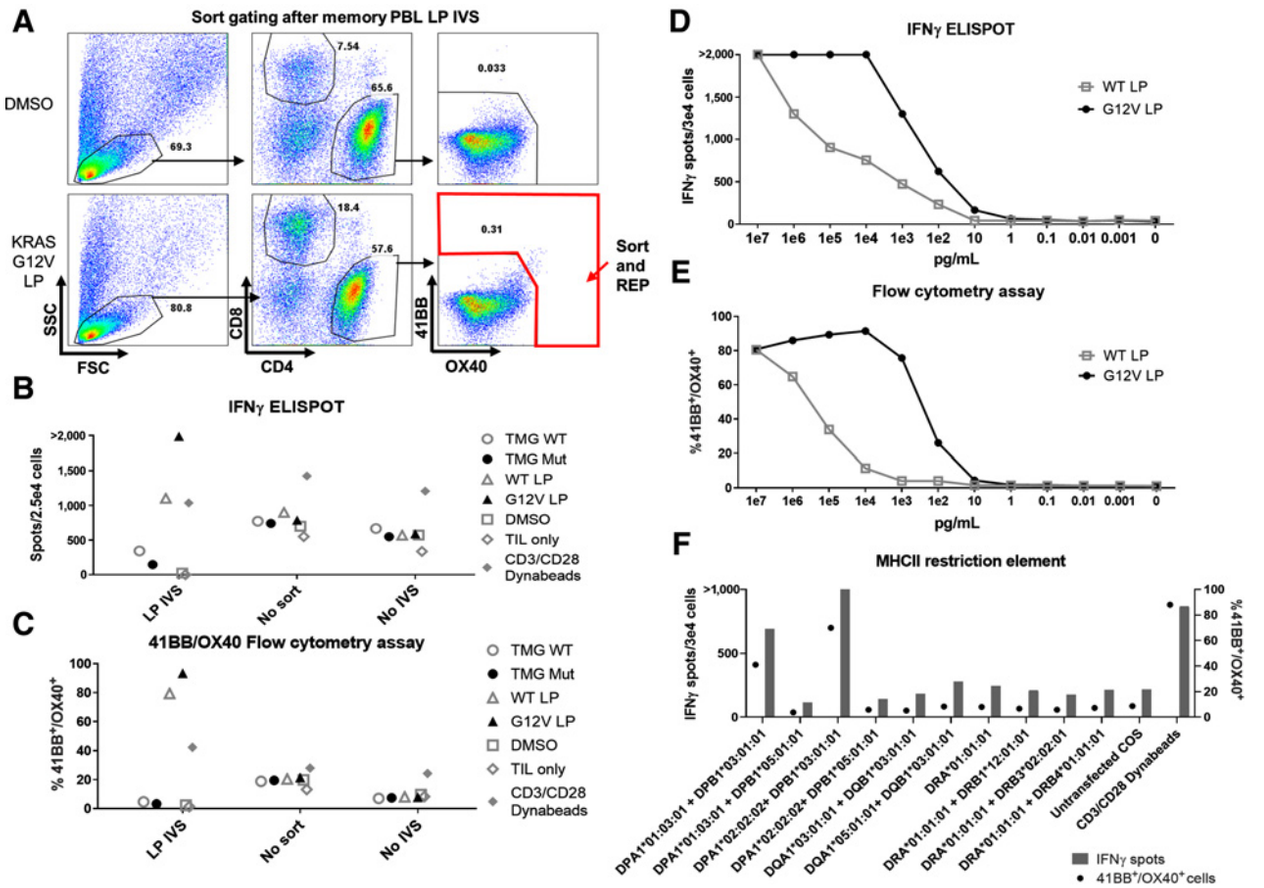

Figure 3.

TCR discovered by PBL IVS. PBL were sorted into CD4 or CD8 memory and effector T cells and IVS with DCs loaded with RAS^{G12V} LP. After the stimulation period, T cells were restimulated with the same target cells. **A,** Flow cytometry assay dot plot showing the gating strategy in which CD4 cells were sorted for high expression of OX40 and 41BB surface markers following RAS^{G12V} LP IVS, with DMSO used as a negative control. **B** and **C,** The sorted cells were rapidly expanded (REP) following the IVS protocol (LP IVS), and were tested for reactivity against RAS by coculturing with DC transfected with WT/Mut TMG or loaded with RAS^{G12V}/RAS^{WT} LP or an equivalent amount of DMSO. Cells that were stimulated but did not sort (no sort) or unstimulated cells (no stimulation) were used as a control for the IVS. T cell only and with anti-CD28/CD3 beads used as negative and positive controls, respectively. After overnight coculturing, cells were analyzed for IFNγ ELISpot (**B**) and 41BB/OX40 **(C)** surface marker upregulation in the live/$CD3^+$/$CD4^+$ gated population by flow cytometry analysis. **D** and **E,** CD4 cells after RAS^{G12V} LP IVS (including one REP after sorting) were tested for avidity to RAS^{G12V}. The cells were cocultured with DCs loaded with RAS^{G12V}/RAS^{WT} LP at various concentrations. After overnight coculturing, cells were analyzed via IFNγ ELISpot (**B**) and 41BB/OX40 (**C**) surface marker upregulation in the live/$CD3^+$/$CD4^+$ gated population by flow cytometry analysis. **F,** The MHC-II restriction element recognized by 4360 CD4 PBL after RAS^{G12V} LP IVS was determined via IFNγ ELISpot (left axis and bars) and 41BB/OX40 flow cytometry assay (right axis and circles). The cells were cocultured with COS7 transfected with DNA plasmids containing the different combinations of the patient's MHC-II α and β chains and loaded with RAS^{G12V} LP.

A Deep-sequencing (Adaptive-biotechnologies):

	TCRB CDR3 Amino Acid	4360-CD4 PBL after LP IVS	4360-1_F1_FrTu	4360-2_F16_FrTu	4360-2_F17_FrTu	4360-2_F9_FrTu	Present In
TCR1	CSASRGATGQPQHF	0.96094004	0	0	0	5.705E-05	1
TCR2	CASSSGTGVAEAFF	0.03846949	0	0	0	0	0

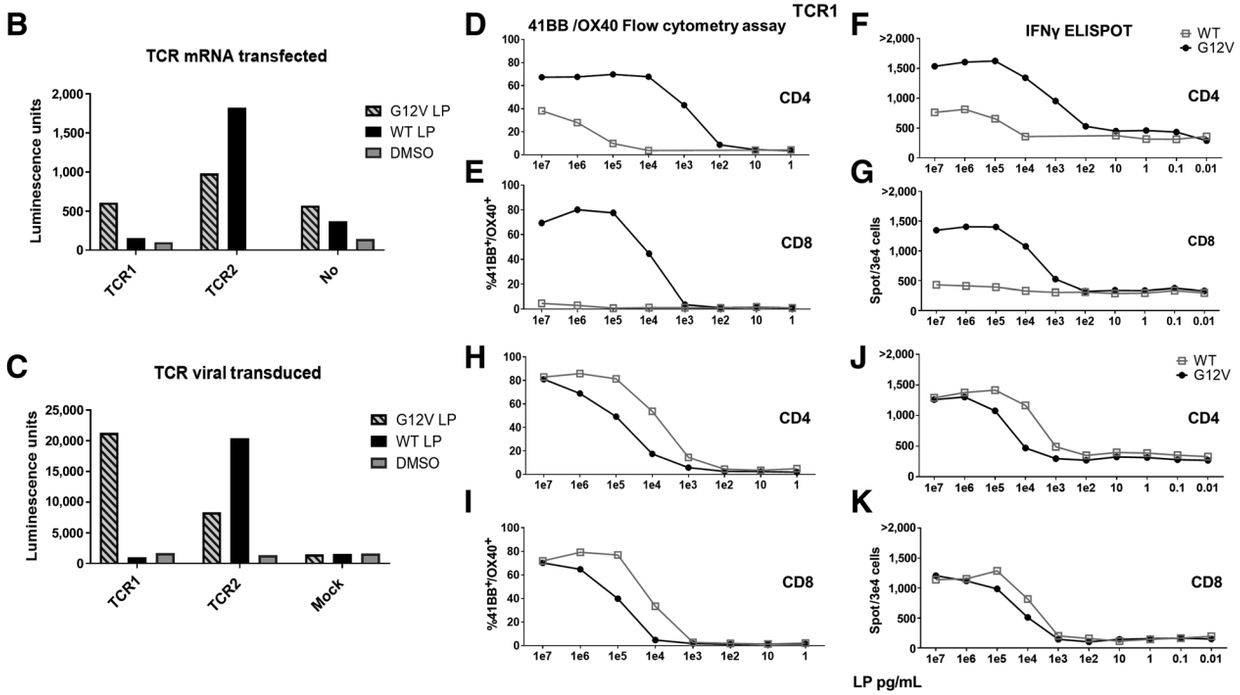

Figure 4.

4360 TCRs recognized RAS hotspot mutation: validation, avidity, and reactivity. **A–K,** Two TCRs (TCR1, TCR2) identified from patient 4360 CD4 PBL after LP IVS single-cell sequencing. **A,** Deep sequencing (Adaptive Biotechnologies) of DNA extracts from four tumor fragments (FrTu) revealed TCR1 existed in one of these fragments (5.7 repeats in 100,000 cells) while TCR2 did not exist in any. **B,** Both TCRs were mRNA transfected or **C,** virally transduced into a Jurkat-CD4-NFAT-Luciferase cell line and then cocultured with DC loaded with RAS^{G12V}/RAS^{WT} LP or the equivalent amount of DMSO. Luciferase activity was measured and presented in Luminescence units. TCR1 (**D–G**) and TCR2 (**H–K**) were virally transduced into patient 4360 PBLs. The cells were enriched to $CD3^+/CD4^+$ cells (**D**, **F**, **H**, **J**) or enriched to $CD3^+/CD8^+$ cells (**E, G, I, K**). The transduced cells were cocultured with DCs loaded with different concentrations of RAS^{G12V}/RAS^{WT} LP. TCR avidity in live/$CD3^+$/$mTCR^+$ cells was analyzed by fow cytometry for 41BB/OX40 surface marker upregulation (**D**, **E**, **H**, **I**) and IFNγ ELISpot (**F**, **G**, **J**, **K**).

lines transfected with DNA plasmids encoding the MHC-II α and β chains of patient 4360 and loaded with RAS^{G12V} LP. Results showed that the recognition was restricted to DPB1*03:01. Interestingly, reactivity was seen when DPB1*03:01 was cotransfected with either DPA1*01:03 or DPA1*02:02 (**Fig. 3F**). In the United States, about 20% of the Caucasian population has the DPB1*03:01 allele (Allele Frequency Net Database: allelefrequencies.net). Reactive cells were sorted and single-cell sequencing resulted in the identification of two candidate reactive TCRs (TCR1 and TCR2). Deep sequencing of four tumor fragments (Adaptive Biotechnologies) showed that the TCR1 (CDR3 β chain) sequence was detected in only one of the tumor fragments at the frequency of 5.7×10^{-5} (specific TCR in total TCRs), whereas TCR2 was not detected in any of the tested tumor fragments (**Fig. 4A**). These two TCRs were tested in a reporter system (see Materials and Methods and ref. 45). The TCRs were either IVT RNA-transfected or retrovirally transduced into Jurkat cells containing the Luciferase reporter gene under the regulation of NFAT and cocultured with DCs loaded with the RAS^{G12V} or RAS^{WT} LP. Luciferase activity showed that TCR1 specifically recognized the RAS^{G12V}-mutated peptide, whereas TCR2 had higher specificity to the RAS^{WT} peptide (**Fig. 4B** and **C**). These results were supported by carrying out peptide titration assays of autologous PBLs that were enriched for CD4 or CD8 cells, followed by transduction of the 4360 TCRs (**Fig. 4D–K**). These results showed that TCR1 is highly specific against the RAS^{G12V} LP-loaded autologous DCs, and indicated that this reactivity was partly CD4 coreceptor dependent (**Fig. 4D–G**). Overall, by using the PBL IVS method, mutated RAS-specific reactivity was found in 3 of 7 patients in whom this reactivity was not previously detected by TIL fragment screening (Supplementary Table S2).

Our current clinically relevant and validated TCRs recognizing a RAS mutation in high avidity are presented here in tables: one for CD8 (**Table 1**) and for CD4 (**Table 2**) cell recognition. This library of TCRs against RAS mutations has the potential for use as off-the-shelf reagents for patient treatment. Among patients having *RAS*-mutated cancers, at least one TCR (CD4 or CD8) is available for use in treatment for about 45% of the Caucasian and about 60% of the Asian populations in the United States. Further data regarding receptors' sequences and antigens are also available (Supplementary Table S6).

Table 1. CD8-validated TCR-recognizing RAS hotspot mutation, available for allogeneic treatment.

RAS mutation	# TCRs discovered	HLA-I restriction	% of individuals that have the allele (Allele Frequency). *Asian population	% Patients eligible for treatment. *Asian population	Minimal epitopes	Patient number	Method	Cancer diagnosis	References
KRAS p.G12D (35%)	1	C*08:02	8% (4.2%)	2.8	GADGVGKSA	3995	TIL screening	Colon	17
	4	C*08:02	8% (4.2%)	2.8	GADGVGKSA (3 TCRs)\ GADGVGKSAL (1 TCR)	4095	TIL screening	Colon	17
	1	A*11:01	14% (7%), *>30%	4.9 *>10.5	VVVGAGGDGK	4373	TIL screening	Colon	
KRAS p.G12V (24%)	1	A*11:01	14% (7%), *>30%	3.36 *>7.2	VVGAVGVGK	4148	PBL IVS	Endometrial	41
	1	C*01:02	5.3% (2.6%), *>30%	1.27 *>7.2	AVGVGKSAL	4391	TIL screening	Colon	
	1	C*01:02	5.3% (2.6%), *>30%	1.27 *>7.2	AVGVGKSAL	4394	TIL screening	Colon	
	1	C*01:02	5.3% (2.6%), *>30%	1.27 *>7.2	AVGVGKSAL	4385	TIL screening	Colon	
				12.4*>27.5					

Note: CD8 TCR Supplementary table showing columns (from left to right): the hotspot mutation recognized by the TCR and the percentage of this mutation among RAS-mutated cancer patients; number of TCRs discovered from the same patient recognizing the same target; the HLA-I restriction each TCR recognizes; percentage of the allele frequency (taken from allelefrequencies.net) and calculation of the percentage of the individuals in the Caucasian or Asian populations (*); percentage of patients eligible for treatment, calculated by multiplying the frequency of individuals that have the allele with the frequency of this RAS mutation (as in the first column) with the sum of percentages from all TCRs (the bottom of this column); ME sequence recognized by the TCR; patient number; the method used to find the TCR (TIL screen/PBL IVS); patient cancer diagnosis in which TCR was found; reference if the TCR has been published before and, if so, where.

Discussion

ACT using autologous TILs can mediate objective responses in about half of patients with metastatic melanoma, including a quarter with durable complete responses (7, 9). As described elsewhere, this method involves the excision of a metastatic tumor and culture of tumor fragments in the presence of IL2 to enable the growth of TILs. After adequate growth occurs, these TILs are tested for recognition of tumor antigens by either coculture with autologous DCs pulsed with peptide pools or transfection with mRNA encoding mutations identified from the whole-exome sequencing of the patient's tumor. Using this method, we found T-cell reactivity in about 80% of patients with metastatic cancers across multiple histologies that include melanoma, colon, pancreas, ovary, and breast (4, 8, 13, 15, 18). However, this process can fail to identify reactivities to antigens recognized by a low percentage of T cells.

RAS mutations can potentially serve as good targets for immunotherapies because the mutations are usually in hotspot mutations and are common among cancer patients with various types of cancers (19–28). We have previously detected T-cell reactivity against RAS hotspot driver mutations and identified the accompanying TCRs from reactive TILs from 3 patients (17, 52). We also showed that administration of TILs targeting a *KRAS* mutation could induce the regression of metastatic cancer in a patient with colon cancer who is now living disease-free over 4 years later (17).

Here, we are describing an efficient and sensitive means to identify anti-RAS reactivities using two methods established in our lab. Unlike our previous screening of TIL fragments against all somatic mutations, here the TIL screening and stimulations were performed specifically against the known *RAS* hotspot mutations by using available and validated reagents specifically for *RAS* mutations. By using this method, we found that 25% (5/20) of newly screened patients had TIL reactivity to a RAS hotspot mutation (Supplementary Table S1.).

A second method, employing a PBL IVS approach, enabled the identification and isolation of additional RAS-reactive T cells that were present at very low frequencies in PBLs of patients with metastatic cancer (41). Using the PBL IVS method, we were able to identity RAS reactive T cells in 43% (3/7) of the patients tested. Notably, these reactivities to RAS were not found by screening TIL (Supplementary Table S2). An advantage of identifying TCRs from PBL is that it does not require invasive procedures to harvest patients' tumor lesions and thus it also helps reduce the time needed to produce a cell product for treatment (50).

We previously showed that administration of PBL retrovirally transduced with TCRs targeting MART-1 or gp100 melanocyte/melanoma antigens can mediate regression in patients with metastatic melanoma (53). In addition, we demonstrated that the transduction of a TCR targeting the NY-ESO-1, a cancer germline antigen, could mediate regression of metastatic synovial cell sarcomas (54, 55). An advantage of using PBLs transduced with TCRs is the ability to create less differentiated effector cells. This contrasts with the senescent state of antigen-reactive TILs where the effector cells have been repetitively stimulated by antigen *in vivo* and have lost much of their proliferative and effector potential.

Because all T cells underwent negative selection in the thymus, TCRs discovered from human T cells are less likely to recognize patient self-antigens. However, IVS method has a risk of producing *de novo* reactivity that did not previously exist *in vivo* and might generate T cells with TCRs that recognized normal as well as TCs. To address this risk, the cells used for IVS were solely memory cells. These cells had already been stimulated *in vivo* and likely differentiated and

Table 2. CD4-validated TCR-recognizing RAS hotspot mutation, available for allogeneic treatment.

RAS mutation	# TCRs discovered	HLA-II restriction	% of individuals that have the allele (Allele Frequency)	% Patients eligible for treatment	Patient number	Method	Cancer diagnosis	References
KRAS p.G12D (35%)	6	DRB3*02	32% (*16.6% U.S. San Francisco Caucasian)	11.2	4238	PBL IVS	Colon	41, 51
KRAS p.G12V (24%)	1	DRB1*07:01	25.5% (14.5%)	6.12	4148	TIL screening	Endometrial	52
	1	DPB1*03:01	20% (10%)	4.8	4360	PBL IVS	Colon	
	1	DRB1*01:01	18% (9%)	4.32	4304	TIL screening	Colon	
KRAS p.G13D (13%)	2	DQA1*05:01/DQB1*03:01	35.1% (19.1%)	4.55	4400	TIL screening	Colon	
KRAS p.G12R (3%)	1	DQA1*05:05(05:01)/DQB1*03:01	35.1% (19.1%)	1.05	4268	TIL screening	Colon	
	1	DRB5*01	35% (*18% U.S. San Francisco Caucasian)	1.05	4270	TIL screening	Pancreatic	
				33.09				

Note: CD4 TCR Supplementary table showing columns (from left to right): the hotspot mutation recognized by the TCR and the percentage of this mutation among RAS-mutated cancer patients; number of TCRs discovered from the same patient recognizing the same target; the HLA-II restriction each TCR recognizes; percentage of the allele frequency (taken from allelefrequencies.net) and calculation of the percentage of the individuals in the Caucasian or subpopulations (*); percentage of patients eligible for treatment, calculated by multiplying the frequency of individuals that have the allele with the frequency of this RAS mutation (as in the first column) with the sum of percentages from all TCRs (the bottom of this column); patient number; the method used to find the TCR (TIL screen/PBL IVS); patient cancer diagnosis in which TCR was found; reference if the TCR has been published before and, if so, where.

proliferated following infection or malignancy. Addition to the higher chance of finding a reactive cell, it is less likely that *de novo* reactivity will be generated by using this IVS approach. Using our methods, the TCRs were discovered using TIL or memory T cells that by definition developed naturally by the patient *in vivo*. This approach is, therefore, less likely to recognize self-antigens compared with the use of normal healthy donors as described by others (56, 57). The TCRs identified through IVS of PBL from patient 4360 failed to recognize autologous APC pulsed with RAS WT peptides. In addition, through deep sequencing of tumor fragments we detected mutant RAS–reactive TCR1 at low concentrations, further supporting that the IVS we performed did not introduce a *de novo* reactivity but rather enriched the RAS-reactive TILs that preexisted. Our data showed that PBLs expressing anti-mutant RAS TCRs specifically recognized not only the autologous patient-derived tumor cell line but also allogenic tumor cell lines with matching MHC restriction and *RAS* mutation, which suggests that these TCRs can potentially be used as "off-the-shelf" reagents for immunotherapy (**Fig. 3D**). Further studies are needed to demonstrate their ability to treat tumor cells *in vivo*.

The library of TCRs presented here are those that were identified to have strong avidity to mutant RAS and little to no self or RAS WT recognition. We focused on RAS^{G12D}/RAS^{G12V} mutations because they are the most common; however, we also successfully isolated TCRs targeting less common RAS^{G13D} and RAS^{G12R}. Taken together, among patients with cancer whose tumor cells contain a *RAS* mutation (about 30% of all patients with cancer), about 45% of the Caucasian and about 60% of the Asian populations in the United States could potentially benefit from the RAS-specific TCR library we have developed. In on-going research, we are attempting to identify additional TCRs that can be used to treat additional populations. We have recently received permission to treat patients with the allogeneic anti-mutant RAS TCRs from the TCR library described in this article under the NCI clinical protocol (NCI-18-C-0049) and are making all TCR sequences we have identified in this report now widely available.

Authors' Disclosures

N. Levin reports patents for 62/981,856, 62/976,655, and 62/975,544 issued, licensed, and with royalties paid, as well as patents for 63/052,502 and 63/086,674 issued. R. Yossef reports patents for 62/981,856 and 62/975,544 licensed and with royalties paid. F.J. Lowery reports patents for 63/052,502 and 63/086,674 issued, as well as a patent for 62/976,655 issued, licensed and with royalties paid. S.A. Rosenberg reports patents for for 62/981,856, 62/975,544, and 62/976,655 issued, licensed, and with royalties paid, as well as patents for 63/052,502 and 63/086,674 issued. No disclosures were reported by the other authors.

Authors' Contributions

N. Levin: Conceptualization, software, formal analysis, supervision, validation, investigation, visualization, methodology, writing–original draft. **B.C. Paria:** Software, formal analysis, investigation. **N.R. Vale:** Formal analysis, investigation. **R. Yossef:** Conceptualization, formal analysis, writing–review and editing. **F.J. Lowery:** Formal analysis, investigation. **M.R. Parkhurst:** Formal analysis, investigation, project administration. **Z. Yu:** Formal analysis, validation, investigation. **M. Florentin:** Formal analysis, investigation. **G. Cafri:** Conceptualization, formal analysis, methodology. **J.J. Gartner:** Resources, data curation, software, formal analysis, validation. **M.L. Shindorf:** Formal analysis, writing–review and editing. **L.T. Ngo:** Formal analysis, investigation. **S. Ray:** Formal analysis. **S.P. Kim:** Conceptualization, formal analysis, writing–review and editing. **A.R. Copeland:** Formal analysis. **P.F. Robbins:** Conceptualization, supervision, validation, writing–review and editing. **S.A. Rosenberg:** Conceptualization, resources, supervision, funding acquisition, validation, writing–review and editing.

Acknowledgments

This work was funded by NCI and Cooperative R&D Agreements (CRADA) and Kite Pharma. The authors thank the NCI Surgery Branch TIL laboratory for growing

TILs. The authors thank Arnold Mixon and Shawn Farid for their assistance with FACS. The authors thank Alicia A. Livinski at the NIH Library Writing Center for manuscript editing assistance.

The publication costs of this article were defrayed in part by the payment of publication fees. Therefore, and solely to indicate this fact, this article is hereby marked "advertisement" in accordance with 18 USC section 1734.

Note

Supplementary data for this article are available at Clinical Cancer Research Online (http://clincancerres.aacrjournals.org/).

Received March 5, 2021; revised April 24, 2021; accepted June 15, 2021; published first June 24, 2021.

References

1. Rosenberg SA, Restifo NP. Adoptive cell transfer as personalized immunotherapy for human cancer. Sci Rev 2015;348:62–8.
2. Rohaan MW, Wilgenhof S, Haanen JBAG. Adoptive cellular therapies: the current landscape. Virchows Arch 2019;474:449–61.
3. Waldman AD, Fritz JM, Lenardo MJ. A guide to cancer immunotherapy: from T cell basic science to clinical practice. Nat Rev Immunol 2020;20: 651–68.
4. Tran E, Robbins PF, Rosenberg SA. 'Final common pathway' of human cancer immunotherapy: targeting random somatic mutations. Nat Immunol 2017;18: 255–62.
5. Linnemann C, van Buuren MM, Bies L, Verdegaal EME, Schotte R, Calis JJA, et al. High-throughput epitope discovery reveals frequent recognition of neo-antigens by CD4+ T cells in human melanoma. Nat Med 2015;21: 81–5.
6. Tran E, Turcotte S, Gros A, Robbins PF, Lu YC, Dudley ME, et al. Cancer immunotherapy based on mutation-specific CD4+ T cells in a patient with epithelial cancer. Science 2014;344:641–5.
7. Rosenberg SA, Yang JC, Sherry RM, Kammula US, Hughes MS, Phan GQ, et al. Durable complete responses in heavily pretreated patients with metastatic melanoma using T-cell transfer immunotherapy. Clin Cancer Res 2011;17: 4550–7.
8. Robbins PF, Lu YC, El-Gamil M, Li YF, Gross C, Gartner J, et al. Mining exomic sequencing data to identify mutated antigens recognized by adoptively transferred tumor-reactive T cells. Nat Med 2013;19:747–52.
9. Goff SL, Dudley ME, Citrin DE, Somerville RP, Wunderlich JR, Danforth DN, et al. Randomized, prospective evaluation comparing intensity of lymphodepletion before adoptive transfer of tumor-infiltrating lymphocytes for patients with metastatic melanoma. J Clin Oncol 2016;34:2389–97.
10. Besser MJ, Itzhaki O, Ben-Betzalel G, Zippel DB, Zikich D, Kubi A, et al. Comprehensive single institute experience with melanoma TIL: Long term clinical results, toxicity profile, and prognostic factors of response. Mol Carcinog 2020;59:736–44.
11. Besser MJ, Shapira-Frommer R, Itzhaki O, Treves AJ, Zippel DB, Levy D, et al. Adoptive transfer of tumor-infiltrating lymphocytes in patients with metastatic melanoma: intent-to-treat analysis and efficacy after failure to prior immunotherapies. Clin Cancer Res 2013;19:4792–800.
12. Deniger DC, Pasetto A, Robbins PF, Gartner JJ, Prickett TD, Paria BC, et al. T-cell responses to TP53 "Hotspot" mutations and unique neoantigens expressed by human ovarian cancers. Clin Cancer Res 2018;24:5562–73.
13. Lu YC, Yao X, Crystal JS, Li YF, El-Gamil M, Gross C, et al. Efficient identification of mutated cancer antigens recognized by T cells associated with durable tumor regressions. Clin Cancer Res 2014;20:3401–10.
14. Stevanović S, Pasetto A, Helman SR, Gartner JJ, Prickett TD, Howie B, et al. Landscape of immunogenic tumor antigens in successful immunotherapy of virally induced epithelial cancer. Science 2017;356:200–5.
15. Zacharakis N, Chinnasamy H, Black M, Xu H, Lu YC, Zheng Z, et al. Immune recognition of somatic mutations leading to complete durable regression in metastatic breast cancer. Nat Med 2018;24:724–30.
16. Tran E, Ahmadzadeh M, Lu YC, Gros A, Turcotte S, Robbins PF, et al. Immunogenicity of somatic mutations in human gastrointestinal cancers. Science 2015;350:1387–90.
17. Tran E, Robbins PF, Lu YC, Prickett TD, Gartner JJ, Jia L, et al. T-cell transfer therapy targeting mutant KRAS in cancer. N Engl J Med 2016;375:2255–62.
18. Parkhurst MR, Robbins PF, Tran E, Prickett TD, Gartner JJ, Jia L, et al. Unique neoantigens arise from somatic mutations in patients with gastrointestinal cancers. Cancer Discov 2019;9:1022–35.
19. Serebriiskii IG, Connelly C, Frampton G, Newberg J, Cooke M, Miller V, et al. Comprehensive characterization of RAS mutations in colon and rectal cancers in old and young patients. Nat Commun 2019;10:3722.
20. Hobbs GA, Der CJ, Rossman KL. RAS isoforms and mutations in cancer at a glance. J Cell Sci 2016;129:1287–92.
21. Hunter JC, Manandhar A, Carrasco MA, Gurbani D, Gondi S, Westover KD. Biochemical and structural analysis of common cancer-associated KRAS mutations. Mol Cancer Res 2015;13:1325–35.
22. Stolze B, Reinhart S, Bulllinger L, Frohling S, Scholl C. Comparative analysis of KRAS codon 12, 13, 18, 61, and 117 mutations using human MCF10A isogenic cell lines. Sci Rep 2015;5:8535.
23. Kodaz H, Osman K, Muhammet B, Hacioglu MB, Bulent E, Cagnur EK, et al. Frequency of RAS mutations (KRAS, NRAS, HRAS) in human solid cancer. Eur J Med Oncol 2017;1:1–7.
24. Biankin AV, Waddell N, Kassahn KS, Gingras M-C, Muthuswamy LB, Johns AL, et al. Pancreatic cancer genomes reveal aberrations in axon guidance pathway genes. Nature 2012;491:399–405.
25. Prior IA, Lewis PD, Mattos C. A comprehensive survey of Ras mutations in cancer. Cancer Res 2012;72:2457–67.
26. Lennerz JK, Stenzinger A. Allelic ratio of KRAS mutations in pancreatic cancer. Oncologist 2015;20:e8–e9.
27. Choi MH, Mejlænder-Andersen E, Manueldas S, El Jellas K, Steine SJ, Tjensvoll K, et al. Mutation analysis by deep sequencing of pancreatic juice from patients with pancreatic ductal adenocarcinoma. BMC Cancer 2019;19:11.
28. Murugan AK, Grieco M, Tsuchida N. RAS mutations in human cancers: Roles in precision medicine. Semin Cancer Biol 2019;59:23–35.
29. Tate JG, Bamford S, Jubb HC, Sondka Z, Beare DM, Bindal N, et al. COSMIC: the catalogue of somatic mutations in cancer. Nucleic Acids Res 2019;47:D941–d7.
30. Smith MJ, Neel BG, Ikura M. NMR-based functional profiling of RASopathies and oncogenic RAS mutations. Proc Natl Acad Sci U S A 2013;110:4574–9.
31. Krasinskas AM, Moser AJ, Saka B, Adsay NV, Chiosea SI. KRAS mutant allele-specific imbalance is associated with worse prognosis in pancreatic cancer and progression to undifferentiated carcinoma of the pancreas. Mod Pathol 2013;26: 1346–54.
32. Grant AD, Vail P, Padi M, Witkiewicz AK, Knudsen ES. Interrogating mutant allele expression via customized reference genomes to define influential cancer mutations. Sci Rep 2019;9:12766.
33. Patricelli MP, Janes MR, Li L-S, Hansen R, Peters U, Kessler LV, et al. Selective inhibition of oncogenic KRAS output with small molecules targeting the inactive state. Cancer Discov 2016;6:316–29.
34. Porru M, Pompili L, Caruso C, Biroccio A, Leonetti C. Targeting KRAS in metastatic colorectal cancer: current strategies and emerging opportunities. J Exp Clin Cancer Res 2018;37:57.
35. Canon J, Rex K, Saiki AY, Mohr C, Cooke K, Bagal D, et al. The clinical KRAS (G12C) inhibitor AMG 510 drives anti-tumour immunity. Nature 2019;575: 217–23.
36. Hughes MS, Yu YYL, Dudley ME, Zheng Z, Robbins PF, Li Y, et al. Transfer of a TCR gene derived from a patient with a marked antitumor response conveys highly active T-cell effector functions. Hum Gene Ther 2005;16:457–72.
37. Morgan RA, Dudley ME, Wunderlich JR, Hughes MS, Yang JC, Sherry RM, et al. Cancer regression in patients after transfer of genetically engineered lymphocytes. Science 2006;314:126–9.
38. Grupp SA, Kalos M, Barrett D, Aplenc R, Porter DL, Rheingold SR, et al. Chimeric antigen receptor-modified T cells for acute lymphoid leukemia. N Engl J Med 2013;368:1509–18.
39. Rosati S, Parkhurst M, Hong Y, Zheng Z, Feldman S, Rao M, et al. A novel murine T-cell receptor targeting NY-ESO-1. J Immunother 2014;37:135–46.
40. Kochenderfer JN, Dudley ME, Kassim SH, Somerville RP, Carpenter RO, Stetler-Stevenson M, et al. Chemotherapy-refractory diffuse large B-cell lymphoma and indolent B-cell malignancies can be effectively treated with autologous T cells expressing an anti-CD19 chimeric antigen receptor. J Clin Oncol 2015;33:540–9.

41. Cafri G, Yossef R, Pasetto A, Deniger DC, Lu YC, Parkhurst M, et al. Memory T cells targeting oncogenic mutations detected in peripheral blood of epithelial cancer patients. Nat Commun 2019;10:449.
42. Iiizumi S, Ohtake J, Murakami N, Kouro T, Kawahara M, Isoda F, et al. Identification of novel HLA class II-restricted neoantigens derived from driver mutations. Cancers 2019;11:266.
43. Dudley ME, Gross CA, Somerville RP, Hong Y, Schaub NP, Rosati SF, et al. Randomized selection design trial evaluating CD8+-enriched versus unselected tumor-infiltrating lymphocytes for adoptive cell therapy for patients with melanoma. J Clin Oncol 2013;31:2152–9.
44. Pasetto A, Gros A, Robbins PF, Deniger DC, Prickett TD, Matus-Nicodemos R, et al. Tumor- and neoantigen-reactive T-cell receptors can be identified based on their frequency in fresh tumor. Cancer Immunol Res 2016;4:734–43.
45. Paria BC, Levin N, Lowery FJ, Pasetto A, Deniger DC, Parkhurst MR, et al. Rapid identification and evaluation of neoantigen-reactive T-cell receptors from single cells. J Immunother 2021;44:1–8.
46. Cohen CJ, Zhao Y, Zheng Z, Rosenberg SA, Morgan RA. Enhanced antitumor activity of murine-human hybrid T-cell receptor (TCR) in human lymphocytes is associated with improved pairing and TCR/CD3 stability. Cancer Res 2006;66:8878–86.
47. Gros A, Robbins PF, Yao X, Li YF, Turcotte S, Tran E, et al. PD-1 identifies the patient-specific CD8(+) tumor-reactive repertoire infiltrating human tumors. J Clin Invest 2014;124:2246–59.
48. Wang QJ, Yu Z, Griffith K, Hanada K, Restifo NP, Yang JC. Identification of T-cell receptors targeting KRAS-mutated human tumors. Cancer Immunol Res 2016;4:204–14.
49. Dudley ME, Wunderlich JR, Shelton TE, Even J, Rosenberg SA. Generation of tumor-infiltrating lymphocyte cultures for use in adoptive transfer therapy for melanoma patients. J Immunother 2003;26:332–42.
50. Malekzadeh P, Pasetto A, Robbins PF, Parkhurst MR, Paria BC, Jia L, et al. Neoantigen screening identifies broad TP53 mutant immunogenicity in patients with epithelial cancers. J Clin Invest 2019;129:1109–14.
51. Cafri G, Gartner JJ, Zaks T, Hopson K, Levin N, Paria BC, et al. mRNA vaccine–induced neoantigen-specific T cell immunity in patients with gastrointestinal cancer. J Clin Invest 2020;130:5976–88.
52. Yossef R, Tran E, Deniger DC, Gros A, Pasetto A, Parkhurst MR, et al. Enhanced detection of neoantigen-reactive T cells targeting unique and shared oncogenes for personalized cancer immunotherapy. JCI Insight 2018;3:e122467.
53. Johnson LA, Morgan RA, Dudley ME, Cassard L, Yang JC, Hughes MS, et al. Gene therapy with human and mouse T-cell receptors mediates cancer regression and targets normal tissues expressing cognate antigen. Blood 2009;114:535–46.
54. Robbins PF, Morgan RA, Feldman SA, Yang JC, Sherry RM, Dudley ME, et al. Tumor regression in patients with metastatic synovial cell sarcoma and melanoma using genetically engineered lymphocytes reactive with NY-ESO-1. J Clin Oncol 2011;29:917–24.
55. Robbins PF, Kassim SH, Tran TLN, Crystal JS, Morgan RA, Feldman SA, et al. A pilot trial using lymphocytes genetically engineered with an NY-ESO-1-reactive T-cell receptor: long-term follow-up and correlates with response. Clin Cancer Res 2015;21:1019–27.
56. Strønen E, Toebes M, Kelderman S, van Buuren MM, Yang W, van Rooij N, et al. Targeting of cancer neoantigens with donor-derived T cell receptor repertoires. Science 2016;352:1337–41.
57. Ali M, Foldvari Z, Giannakopoulou E, Böschen ML, Strønen E, Yang W, et al. Induction of neoantigen-reactive T cells from healthy donors. Nat Protoc 2019;14:1926–43.